100639-1002

DL/SCI/TM30A

technical memorandum Daresbury Laboratory

DL/SCI/TM30A

SOME ASPECTS OF THE DESIGN OF PLANE PERIODIC PERMANENT MAGNETS FOR USE IN UNDULATORS AND FREE ELECTRON LASERS

by

M.W. FAN+, Atomic Energy Institute, Peking,
and
M.W.POOLE and R.P. WALKER, Daresbury Laboratory.

+ Visiting Scientist

LENDING COPY

DECEMBER, 1981

Science & Engineering Research Council

Daresbury Laboratory

Daresbury, Warrington WA4 4AD

1. INTRODUCTION

The design of undulator magnets is receiving considerable attention at a number of laboratories with electron storage rings, including Daresbury. These devices in general have a larger number of poles, shorter magnetic period and smaller magnetic field compared with wiggler magnets and can produce a line spectrum of radiation unlike the continuous spectrum generated in both conventional bending magnets and wigglers. Free electron laser (FEL) experiments are being carried out or have been proposed in a number of countries and a periodic magnet is also the basis of these devices.

Most initial work on periodic magnets[1-3] concentrated on electromagnets with plane geometry or on the alternative helical geometry employing superconducting windings, but more recently the use of rare earth cobalt (REC) permanent magnets has been considered. A permanent magnet undulator has already been built and operated on the SPEAR storage ring at Stanford[4] and similar development work is being undertaken at Brookhaven and Orsay. Free electron laser experiments employing a permanent magnet system have been initiated at Novosibirsk and are under construction at several laboratories in the USA.

In a previous report[5] it was shown that the properties of rare earth cobalt lead to a particularly simple mathematical description involving only surface currents, and a computer program, PMU3D, for carrying out three-dimensional field calculations with periodic magnets was described. Although preliminary guide-lines can be established on the basis of a simple formula which assumes infinite magnet width (i.e. 2D geometry), such a 3D program is necessary in order to produce a final optimised magnet design. In this report the factors influencing the design of a

periodic permanent magnet are first discussed and then the results of computations using PMU3D are presented for a range of realistic magnet geometries. In particular the effects of changing the magnet gap, block height and period on the required block width are discussed. Finally a novel method of improving the field quality of such magnets using shims is described.

2. DESIGN CRITERIA

The choice of magnet parameters is influenced mainly by the required spectral properties - output wavelength, tuning range, number of harmonics and their relative intensity - but in addition a number of other factors have to be taken into account in the design, namely the properties of the available types of REC material, end effects and the practical limitations on the magnet dimensions (not least, cost).

2.1 The Influence of Magnet Parameters on the Spectral Properties

<u>Field amplitude</u>

Figure 1 shows one period of a plane periodic magnet composed of two separate arrays of magnetised blocks. For an infinitely wide magnet a simple expression for the vertical component of magnetic field can be derived analytically:

$$B_y = B_o \cos(kz) \cosh(ky) \tag{1}$$

where the field amplitude is given by[6]:

$$B_o = 2B_r \frac{\sin\pi/M}{\pi/M} (1 - e^{-kh})\, e^{-kg/2} \tag{2}$$

with
- $k = 2\pi/\lambda_o$, λ_o = magnet period
- h = height of blocks
- g = total gap between arrays of blocks
- M = number of blocks per period
- B_r = remanent field of the material

In this report only the component B_y will be considered; this is the only component in the median plane and is the one which determines the major features of the electron trajectories. In a complete three-dimensional treatment a further parameter, the magnet width w, must be included and it will be seen that this also affects the field amplitude.

The radiation produced by an undulator (usually called spontaneous radiation in the case of a FEL) consists of a series of harmonics with wavelengths given by:

$$\lambda_i = \frac{1}{i}\frac{\lambda_o}{2\gamma^2}(1 + K^2/2) \tag{3}$$

where i = harmonic number
γ = relativistic factor

The dimensionless parameter K is given by:

$$K = 93.4\ \lambda_o B_o \qquad (\lambda_o \text{ in m, } B_o \text{ in T}) \tag{4}$$

This factor not only influences the output wavelength but also alters the quality of the spectrum in terms of the number of harmonics and their relative intensity. Thus all magnet parameters are important in determining the nature of the radiation produced by the device. With a given permanent magnet the output wavelength can be tuned only by varying the magnet gap, but this also changes the K value. The amount of tuning required may be one of the criteria which influences the design.

Field homogeneity

The linewidth of the radiation may be important for certain applications. The natural linewidth (width of each harmonic) is given by:

$$\frac{\Delta\lambda}{\lambda_i} = \frac{1}{iN} \tag{5}$$

where N is the number of magnet periods. This is the minimum possible linewidth. In addition there is broadening caused for example by the variation of magnetic field over the finite cross-sectional area of the electron beam:

$$\frac{\Delta\lambda}{\lambda} = \frac{K^2}{(1+K^2/2)}\frac{\Delta B}{B_o} \tag{6}$$

If the electron beam source is a linac, as it may be for a FEL experiment, the transverse dimensions of the beam are relatively large and roughly equal and so broadening due to the field variation in both x and y directions (see fig.1) must be taken into account. In an electron storage ring the vertical beam size is usually small but in the horizontal plane it may be significant.

It follows from eqn.(1) that the field close to the co-ordinate origin can be approximated by a quadratic variation in both y and z directions. This may be extended to three dimensions by use of the following general expression which can be obtained from Maxwell's Equations:

$$\nabla^2 B_y = 0 \tag{7}$$

It follows therefore that the field can be expressed as follows:

$$B_y = B_o(1 - a_x x^2)(1 + a_y y^2)(1 - a_z z^2) \tag{8}$$

in which the coefficients a_x, a_y, a_z are all positive. Equation (7) then means that:

$$a_y - a_x - a_z = 0 \tag{9}$$

In the 2D case $a_x = 0$ and from eqn.(1) $a_y = a_z = 0.5(2\pi/\lambda_o)^2$, assuming a purely sinusoidal field variation along the z axis. In 3D all magnet parameters play a part in determining the relative sizes of the three quadratic coefficients and hence the amount of line broadening that will occur.

2.2 Magnet Dimensions

The main restrictions on the overall dimensions of the magnet are the length, which affects the choice of λ_o and N, and the gap. Often a magnet will be required to operate at the minimum gap that will contain the electron beam vacuum vessel and in the case of a FEL perhaps also the output radiation mode. In the future magnets may be designed with the permanent magnet blocks inside the vacuum vessel, and in this case the block height and width will be critical parameters.

2.3 Cost and Properties of Available REC Material

In any design it will be desirable to minimise the cost of the material, which increases in proportion to the total volume required and more rapidly with the value of the remanent field (which for REC will be in the range 0.85-1.05 T). A reduction in remanent field will cause a proportionate change in the field at every point which may have to be offset by a much more costly volume increase, depending on the particular design. It follows from eqn.(2) that the magnet gap should be kept as small as possible in order that the remanent field and block height required to achieve a given B_o value (i.e. K value for given λ_o) can be minimised. The magnet block width will be determined largely by the requirement for a given field homogeneity.

It is difficult to produce blocks magnetised along the diagonal of a side face as required for example if there are 8 blocks per period (M=8), and so all present designs are based on M=4. Normal manufacturing tolerances produce blocks with a variation in the remanent field of ± 5% but this may be reduced at a cost by a selection process. The effect of this variation on the properties of the radiation has yet to receive detailed investigation but clearly it will modify the performance.

2.4 End Effects

The net deflection of an electron beam passing through the magnet must be zero and so the ends of the magnet must be designed appropriately. In the Stanford design[4] rotatable end blocks are used but an alternative scheme is to use blocks of half the normal length at the ends which

automatically guarantees a zero field integral; this will be described in detail in a later report. Some form of compensation coil will also be required for correction of any small residual errors.

3. RESULTS OF COMPUTATIONS USING PMU3D

The design which will be concentrated on has the following parameters:

period	λ_o	= 80 mm
gap	g	= 25 mm
block height	h	= 20 mm
block width	w	= 80 mm

The effect of changes in each of these parameters on the field amplitude and homogeneity will be considered in section 3.1. The results of preliminary investigations of a shimming technique are presented in the following section. In the final section the effect of having very large magnet periods on the longitudinal (i.e. along the z axis) distribution of field is considered.

The field in the centre (z=0) of a periodic magnet is influenced by the total number of blocks in the magnet. Computations show that in practice only small changes are produced by adding further blocks when there are at least 1.5 periods on either side of the centre. In order to ensure that the results obtained are not influenced by the finite length of the magnet a sufficiently large number of blocks have been included in all computations reported here.

3.1 Field Amplitude and Homogeneity

Figure 2 shows the variation in B_o with magnet width for the standard geometry and it can be seen that it approaches the value predicted by eqn.(2) in the limit of large width. At w = 80 mm, the field is within 2% of the value for infinite width.

In figs.3, 4 and 5 the variation of B_o with period, gap and block height is shown for widths of 20, 40 and 80 mm together with the result for infinite width from eqn.(2). It can be seen that all dimensions affect the field amplitude with the most rapid variation occurring in each case when the dimension is smallest. In each figure the form of the curves for both finite and infinite width is similar and it appears that there is roughly a constant factor between the two. Figures 6, 7 and 8 examine this in more detail by showing B_o/B_{2D} ,where B_{2D} is the result of eqn.(2), as a function of width at various periods, gaps and block heights. Comparison of these results shows clearly that there are 3D effects dependent on all magnet dimensions but that the effect of finite block width is predominant.

Figure 9 shows the field homogeneity in the x direction defined by

$$\frac{\Delta B}{B_o}(x) = \frac{B(x) - B_o}{B_o}$$

for various magnet widths, with the standard geometry. It can be seen that in general the field quality is very poor; this is because there is no iron to shape the field distribution. As a result relatively large widths are required to meet fairly modest homogeneity requirements. For example, to achieve better than 1% homogeneity over ± 10 mm would require a width of 80 mm.

Figures 10, 11 and 12 show that changes in period, gap and block height all alter the transverse field distribution, the latter having the smallest effect. It can be seen that the homogeneity becomes worse as each of these dimensions increases.

Figures 13 to 16 give the corresponding results for the homogeneity in the y direction which is much worse than in the x direction. Figure 13

shows that increasing the magnet width improves the homogeneity but that a limit is reached at large widths, and fig.14 shows that this depends strongly on magnet period. These results are in agreement with the general conclusions of section 2.1. Figures 15 and 16 demonstrate that variations of gap and block height have a smaller effect and that the homogeneity is worse for large gaps and heights as it is also in the x direction (see figs.11 and 12).

Figures 17 and 18 give the field homogeneity as a function of x and y respectively for the standard geometry together with the quadratic variation predicted by eqn.(8), where a_x and a_y are calculated for small x and y. It can be seen that a quadratic function is a good approximation to the true field distribution over a considerable fraction of the magnet width and gap. The coefficients a_x and a_y may therefore be used as a measure of the field homogeneity over the beam cross-section, provided this is not too large compared with the magnet aperture. Figure 19 shows how these coefficients vary as a function of magnet width for the standard geometry. It can be seen that in the limit of large width a_x becomes very small and a_y is approximately equal to a_z, and these are close to the result of the simple model, $a_y = 0.5\ (2\pi/\lambda_o)^2$, shown dotted. As the width decreases a_z stays roughly constant with the result that a_x and a_y differ by a constant amount. As expected a_y is always the largest term; the homogeneity is worst in the y direction.

In figure 20 the results for a_x and a_y as a function of λ_o are presented at two widths, w = 20 and w = 100. The dotted line is again the simple model. It can be seen that at the larger width the variation of a_y is in good agreement with the simple model. The variation of a_z is not shown since for both widths the curve lies very close to that of a_y at

$w = 100$. The coefficient a_x does not vary greatly with period and so there is almost a constant difference between the two curves for a_y. Figures 21 and 22 are similar graphs of the variation with gap and block height. There is significant variation of a_x and a_y with gap but much less with block height, particularly above $h = 20$ mm.

3.2 Use of Shims

One of the major factors which determines the cost of a permanent magnet undulator is the block width since in general it has to be much greater than the required good field aperture. It is therefore advantageous to use a field shaping technique to improve the field quality and so to allow the block width to be decreased. Figure 23 shows that the homogeneity in the x direction can be improved with the sort of shim used in a conventional dipole electromagnet. Curves 1-4 are for a constant shim width of 10 mm but different shim heights chosen to optimise the field uniformity over ± 20 mm. The geometry is otherwise the standard one with a width of 60 mm. The field homogeneity for widths of 60 mm and 100 mm without shims is shown for comparison. It can be seen that the use of a suitable shim allows the field uniformity requirement to be met with substantially reduced block width. As might be expected such field correction depends critically on the shim height so that the dimensional tolerances in block manufacture need to be as good as ± 0.1 mm.

The effect of changing the magnet gap on the performance of a shim is shown in fig.24. In this example the block width and shim width have been increased to 80 mm and 15 mm respectively and the different curves refer to gaps in the range 42-56 mm for a fixed shim height of 3.7 mm; the associated field amplitude is reduced from 0.19T to 0.11T. It can be seen that the field homogeneity changes significantly with magnet gap but

nevertheless it should be possible to design a shim to meet a particular field uniformity requirement for a range of gaps, provided the variation required is not too great.

3.3 Large Magnet Periods

Equation 2 shows that the field amplitude increases monotonically as the gap decreases or the block height increases but the function $B_o(\lambda_o)$ is more complicated and in fact goes through a maximum at:

$$\lambda_o/g = \frac{2\pi\ h/g}{\ell n(1+2h/g)} \qquad (10)$$

Figure 25 shows B_o as a function of λ_o for widths of 20 mm and 80 mm. These curves are similar in shape to the 2D result which is also shown and have a maximum at about the same value, given by eqn.(10) as $\lambda_o/g = 5.26$. However the value of B_o is not of direct interest, rather a particular K value will be specified, and furthermore in most applications λ_o/g will be restricted to smaller values (typically 1.5-3.0).

At large values of λ_o the field distribution along the axis of the magnet becomes non-sinusoidal as demonstrated in fig.26 which shows B(z) over a complete magnet period for λ_o of 100 mm, 200 mm and 400 mm. It can be seen that for periods greater than 100 mm in this case the field becomes increasingly rich in harmonics. The effect of this on the radiation spectrum has not yet been investigated but it is certain that the power in the fundamental will be reduced at the expense of the higher harmonics. Further study will be required before the results can be generalised to include variations in gap, block height and width.

4. CONCLUSIONS

Three dimensional field calculations have confirmed that all magnet dimensions affect the performance and must therefore be carefully chosen for an optimum design. The effect of finite width modifies the results of the 2D analytic formula for B_o in a non-trivial way. It has been shown that the field inhomogeneity in one direction (a_y) is always greater than that in the perpendicular direction (a_x) by an amount approximately equal to $0.5(2\pi/\lambda_o)^2$. As the width of the magnet increases a_y approaches this limiting value and a_x approaches zero. Thus in the case of a ribbon-like electron beam the larger beam dimension should correspond with the x direction in order to minimise the resulting line broadening. For a circular cross section beam a fundamental limitation exists on the homogeneity that can be achieved which depends on the magnet period, as noted in a previous report on periodic electromagnets[3]. Both the magnet gap and block height can also have an appreciable effect on the field amplitude and the homogeneity in both planes, depending on the parameter range of interest in a particular design.

The technique of adding shims to improve field quality looks promising in principle; however a serious drawback could be the extra cost involved in manufacture and the difficulty in maintaining the required tolerances. Further work would be required to establish the range of gaps that might be possible for a given homogeneity requirement and the associated reduction in the volume of material for an optimised shim design. The effect on the homogeneity in the y direction has not yet been investigated, but it follows from eqn.(9) that it will be simultaneously improved in this plane.

The results described here provide adequate guide lines for the optimised design of any practical three dimensional periodic magnet based on plane arrays of REC material. Further work is however planned on the specialised topic of end effects. Any final design also necessitates a full assessment of the required manufacturing and assembly tolerances.

REFERENCES

1. Proc. Wiggler Workshop, Stanford Report SSRP 77/05, Stanford (1977).

2. Proc. Wiggler Meeting, INFN Frascati (1978).

3. M.W. Poole and R.P. Walker, Nucl. Instrum. Meth. 176 (1980) 487.

4. K. Halbach et al, 1981 Particle Accelerator Conference, IEEE Trans. Nucl. Sci., NS-28 (1981) 3136.

5. M.W. Fan, M.W. Poole and R.P. Walker, DL/SCI/TM/29A.

6. M.W. Poole and R.P. Walker, Proc. 7th Int. Conf. on Magnet Technology (MT7), Karlsruhe 1981, in IEEE Trans. Magnetics, MAG-17, No. 5 (1981) 1978.

FIGURE CAPTIONS

Fig.1 The geometry of an undulator magnet with four blocks per period; only one period is shown.

Field amplitude as a function of:

Fig.2 Width
Fig.3 Period
Fig.4 Gap
Fig.5 Block height

} various widths

Ratio of field amplitude to the 2D result as a function of width:

Fig.6 Various periods
Fig.7 Various gaps
Fig.8 Various heights

Field homogeneity in the x-direction:

Fig.9 Various widths
Fig.10 Various periods
Fig.11 Various gaps
Fig.12 Various heights

Field homogeneity in the y-direction:

Fig.13 Various widths
Fig.14 Various periods
Fig.15 Various gaps
Fig.16 Various heights

Fig.17 Field homogeneity in the x-direction compared with a quadratic function

Fig.18 Field homogeneity in the y-direction compared with a quadratic function

Field homogeneity coefficients as a function of:

Fig.19 Width
Fig.20 Period
Fig.21 Gap
Fig.22 Height

} for w = 20 mm and 100 mm

Fig.23 Field homogeneity in the x-direction for various shim heights

Fig.24 Field homogeneity in the x-direction for various gaps, with a constant shim height

Fig.25 Field amplitude as a function of period for various widths

Fig.26 Field distribution along the z-axis for various periods.

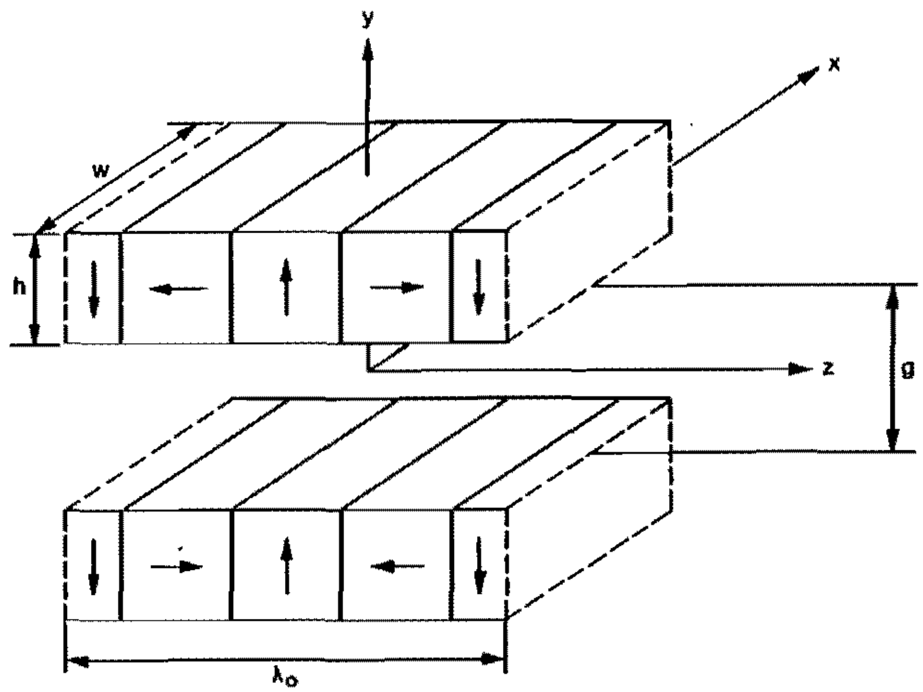

y
x
w
h
z
g
λo

Fig. 1

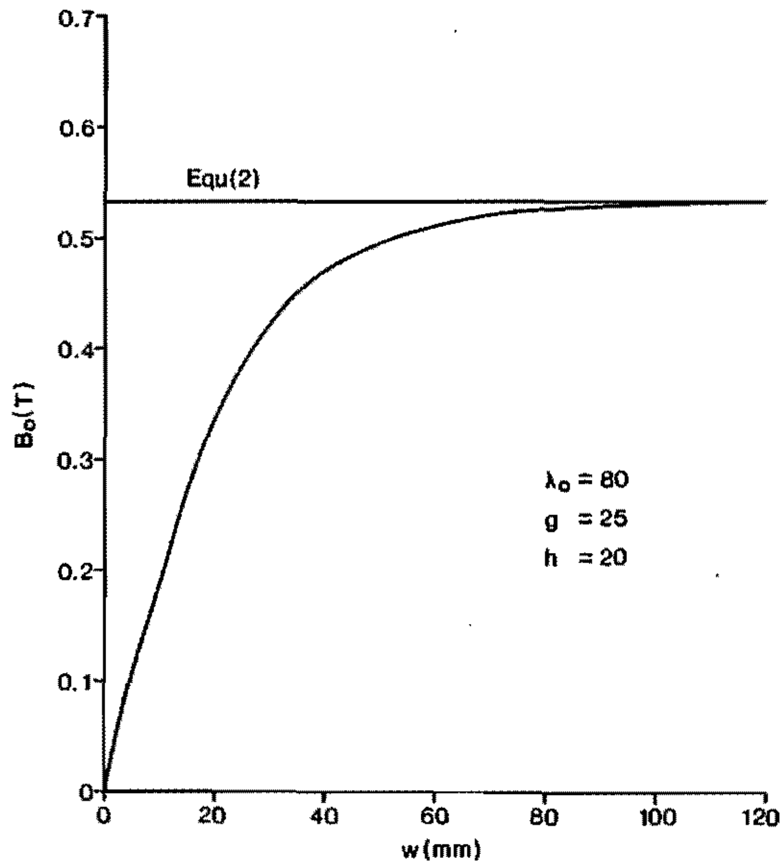

0.7
0.6
0.5
0.4
0.3
0.2
0.1
0
Equ(2)
Bo(T)
λo = 80
g = 25
h = 20
0
20
40
60
80
100
120
w (mm)

Fig. 2

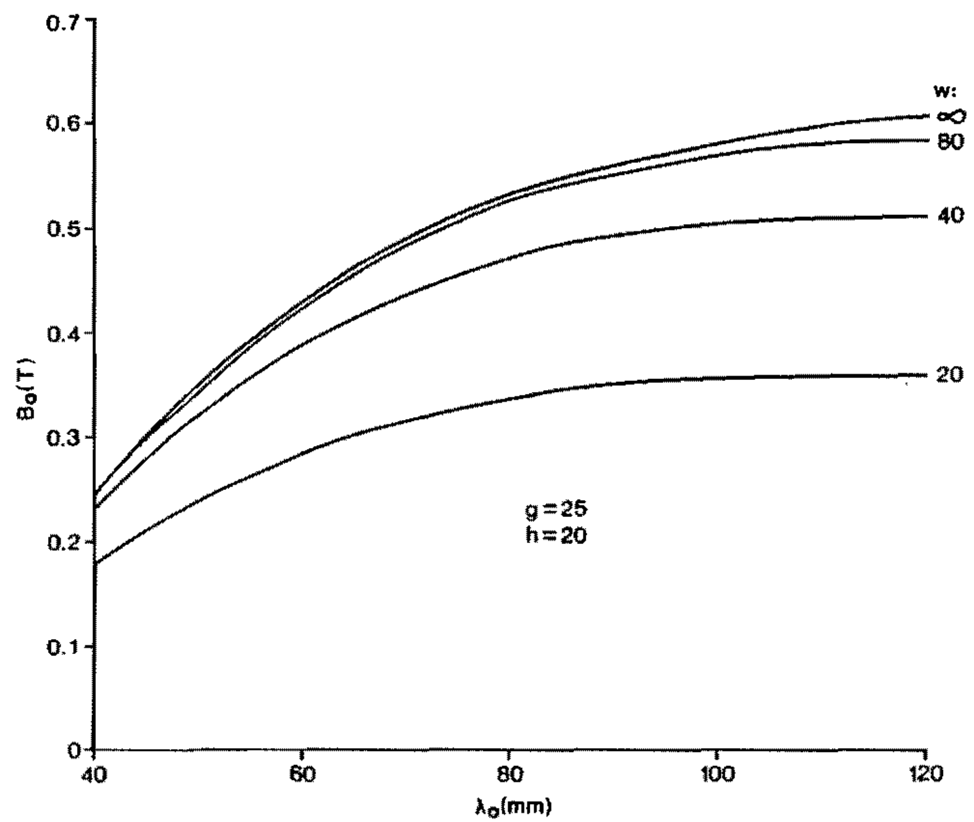
0.7
0.6
0.5
0.4
0.3
0.2
0.1
0
$B_o(T)$
40
60
80
100
120
λ_o(mm)
w:
∞
80
40
20
g = 25
h = 20

Fig. 3

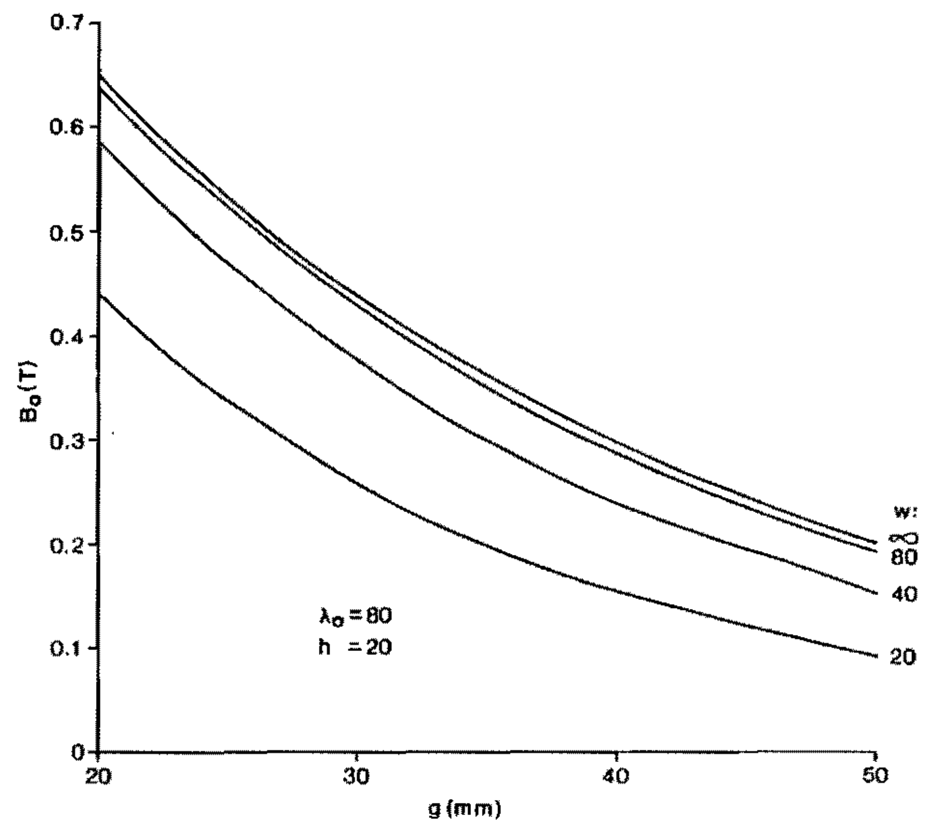
0.7
0.6
0.5
0.4
0.3
0.2
0.1
0
$B_o(T)$
20
30
40
50
g (mm)
w:
∞
80
40
20
λ_o = 80
h = 20

Fig. 4

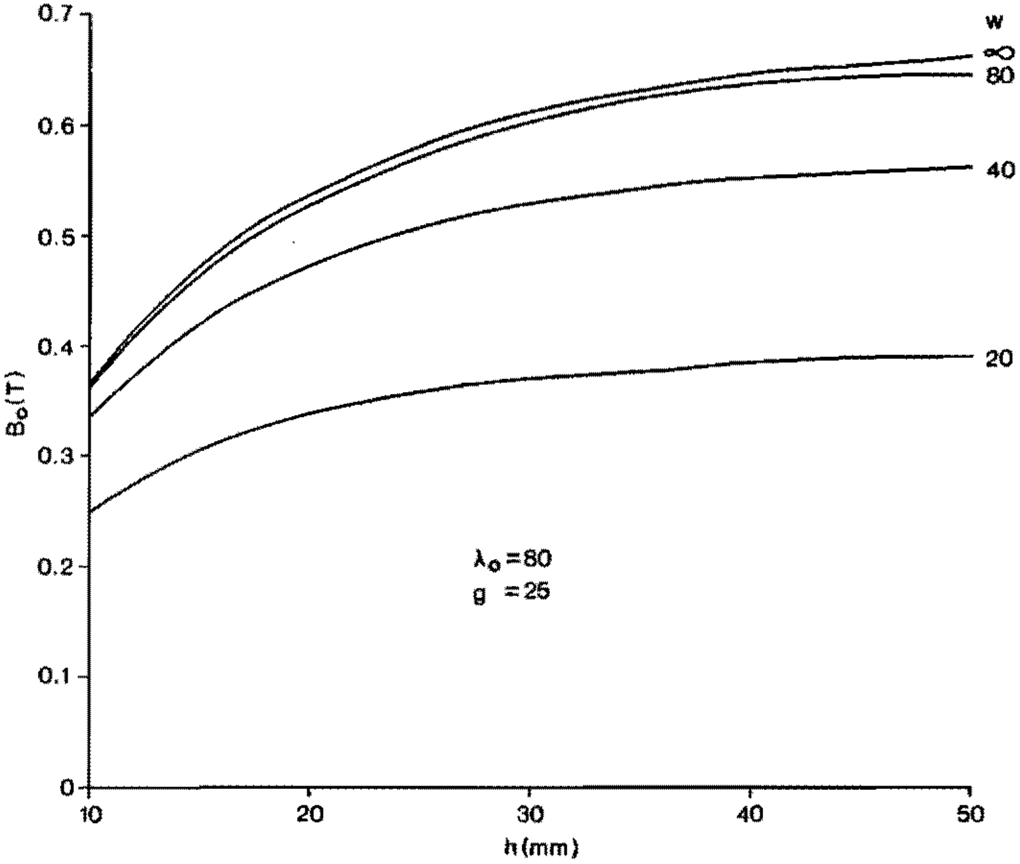

0.7
0.6
0.5
0.4
0.3
0.2
0.1
0
$B_o(T)$
10
20
30
40
50
h (mm)
w
∞
80
40
20
$\lambda_o = 80$
g = 25

Fig. 5

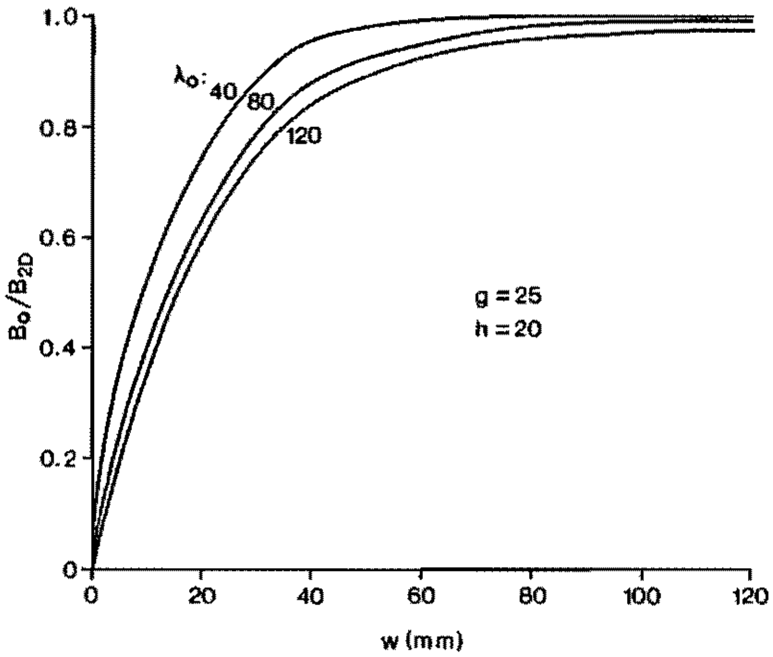

1.0
0.8
0.6
0.4
0.2
0
B_o/B_{2D}
0
20
40
60
80
100
120
w (mm)
λ_o: 40
80
120
g = 25
h = 20

Fig. 6

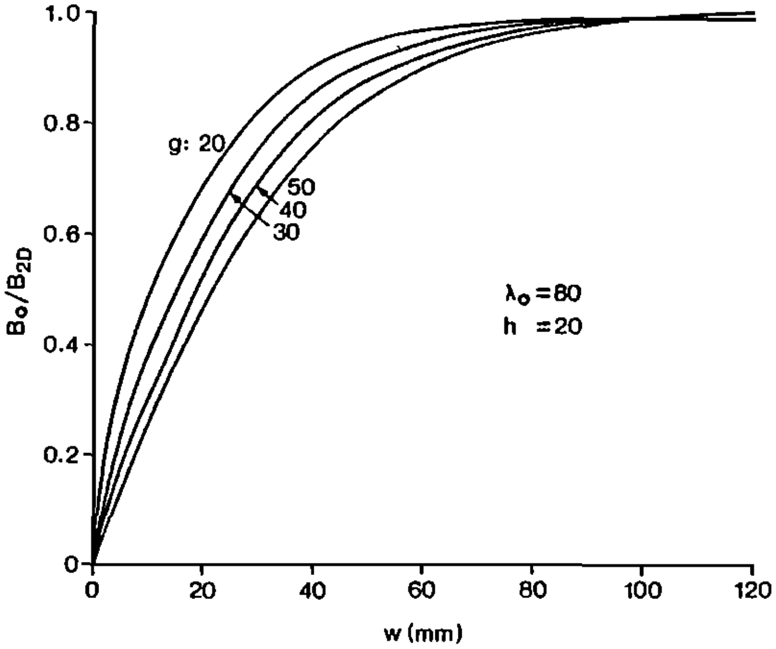
1.0
0.8
0.6
0.4
0.2
0
B_o/B_{2D}
g: 20
50
40
30
$\lambda_o = 80$
h = 20
0
20
40
60
80
100
120
w (mm)

Fig.7

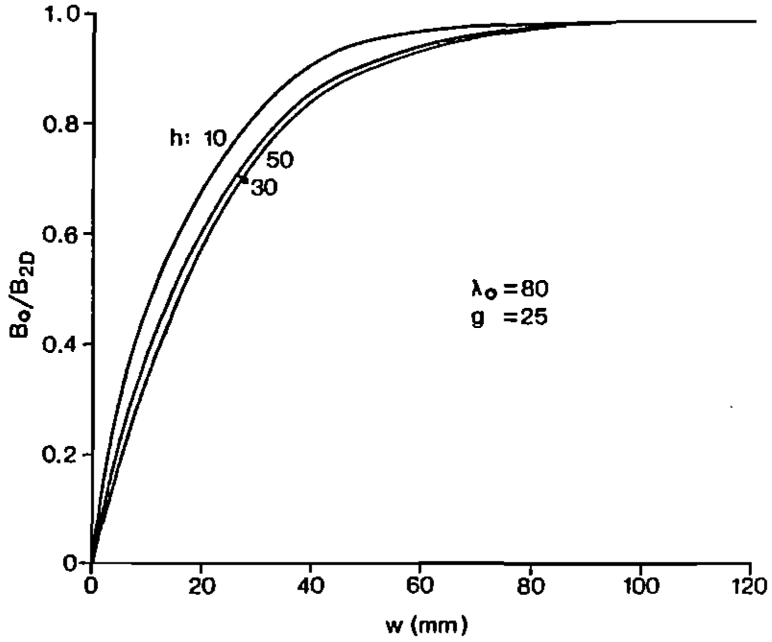
1.0
0.8
0.6
0.4
0.2
0
B_o/B_{2D}
h: 10
50
30
$\lambda_o = 80$
g = 25
0
20
40
60
80
100
120
w (mm)

Fig. 8

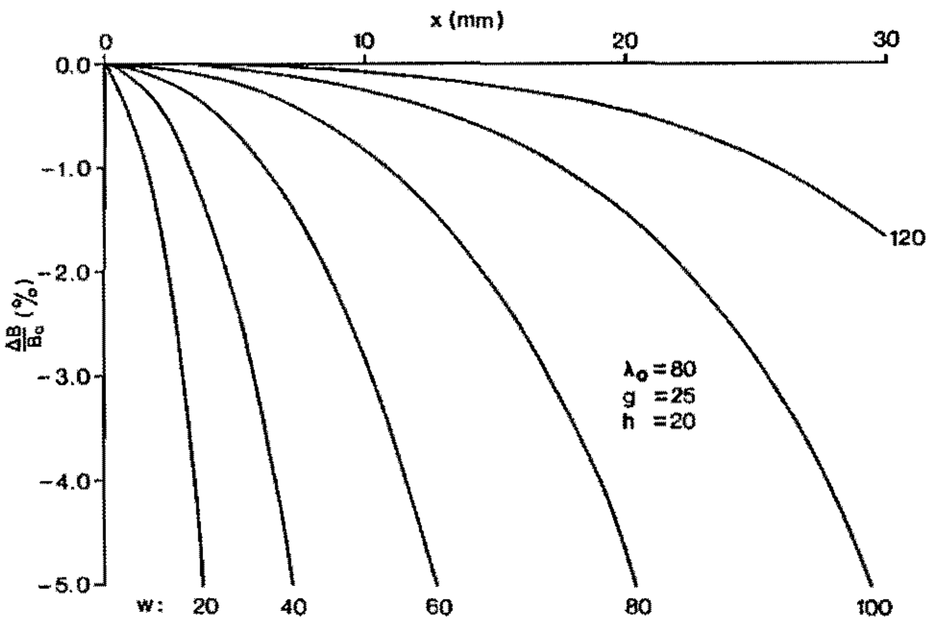

x (mm)
0
10
20
30
0.0
-1.0
-2.0
-3.0
-4.0
-5.0
$\frac{\Delta B}{B_o}$ (%)
120
λ_o = 80
g = 25
h = 20
w: 20 40 60 80 100

Fig. 9

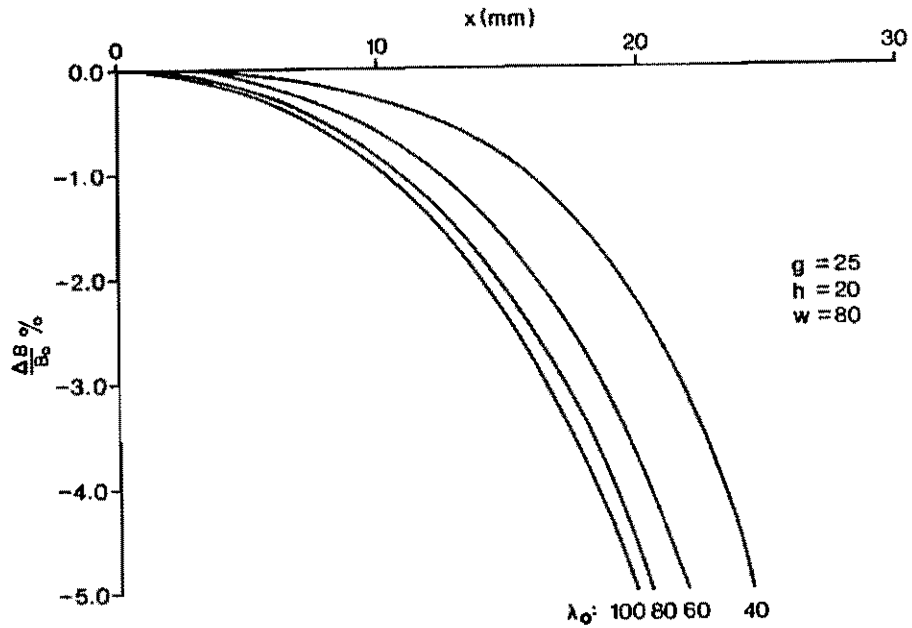

x (mm)
0
10
20
30
0.0
-1.0
-2.0
-3.0
-4.0
-5.0
$\frac{\Delta B}{B_o}$ %
g = 25
h = 20
w = 80
λ_o: 100 80 60 40

Fig. 10

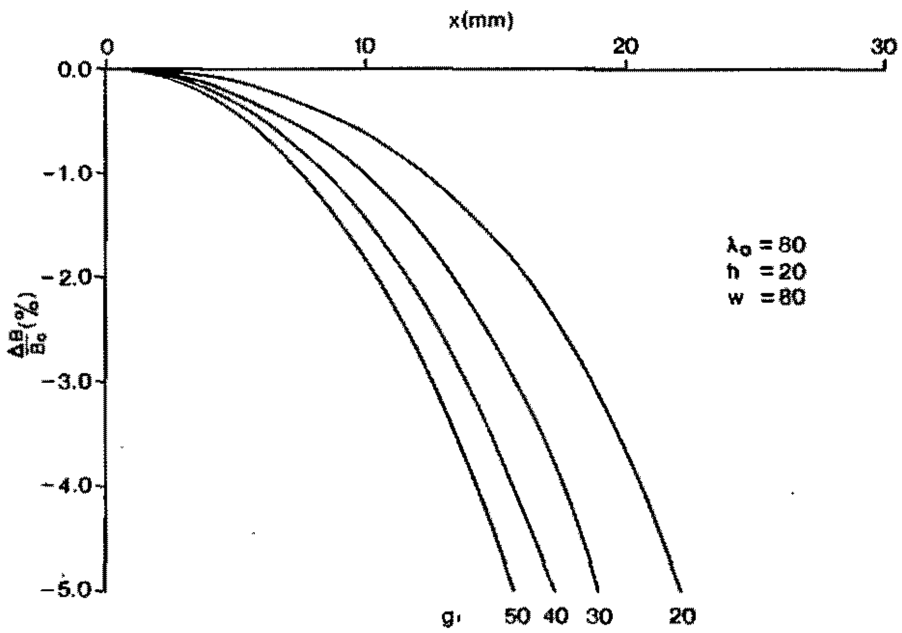
x(mm)
0
10
20
30
0.0
-1.0
-2.0
-3.0
-4.0
-5.0
$\frac{\Delta B}{B_o}$(%)
λ_o = 80
h = 20
w = 80
g: 50 40 30 20

Fig. 11

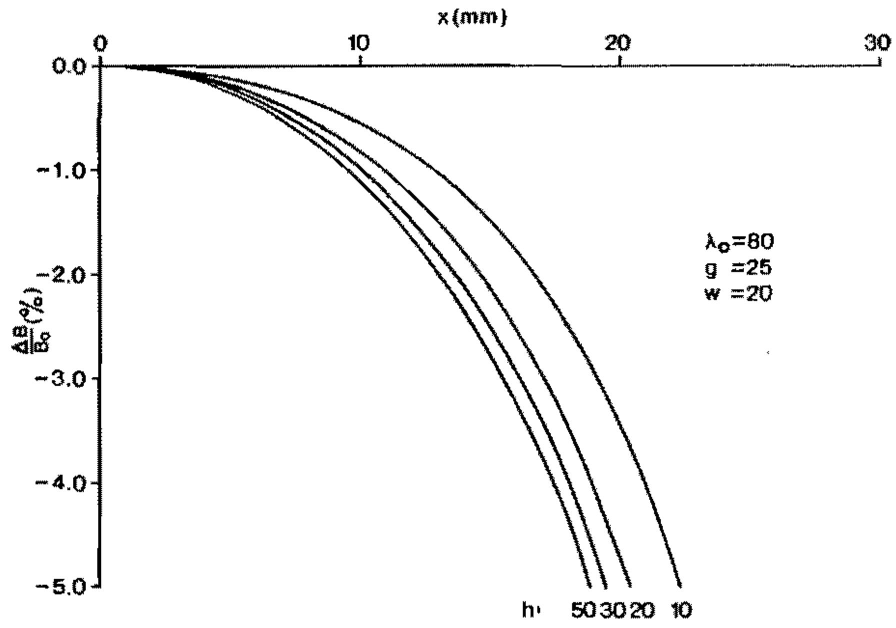
x(mm)
0
10
20
30
0.0
-1.0
-2.0
-3.0
-4.0
-5.0
$\frac{\Delta B}{B_o}$(%)
λ_o=80
g =25
w =20
h: 50 30 20 10

Fig 12

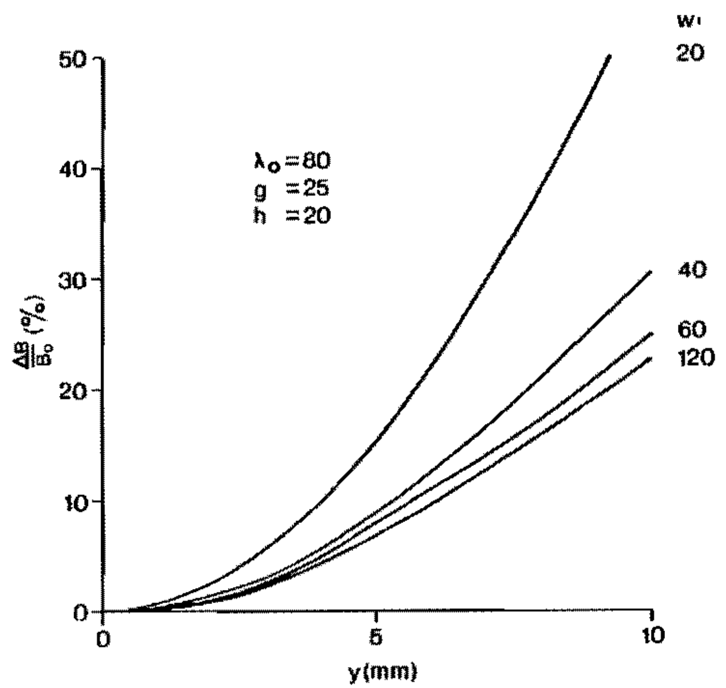
w:
20
40
60
120
$\lambda_o = 80$
g = 25
h = 20
$\frac{\Delta B}{B_o}$ (%)
50
40
30
20
10
0
0
5
10
y(mm)

Fig. 13

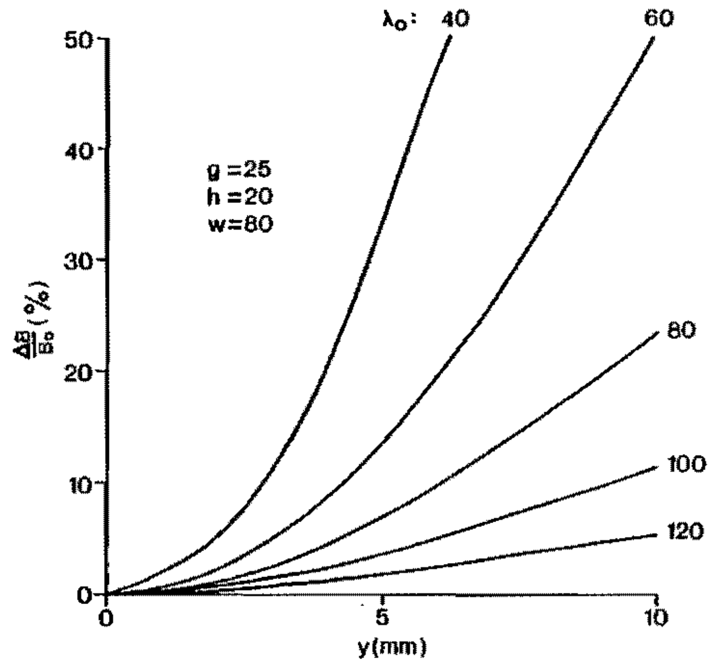
λ_o: 40
60
80
100
120
g = 25
h = 20
w = 80
$\frac{\Delta B}{B_o}$ (%)
50
40
30
20
10
0
0
5
10
y(mm)

Fig. 14

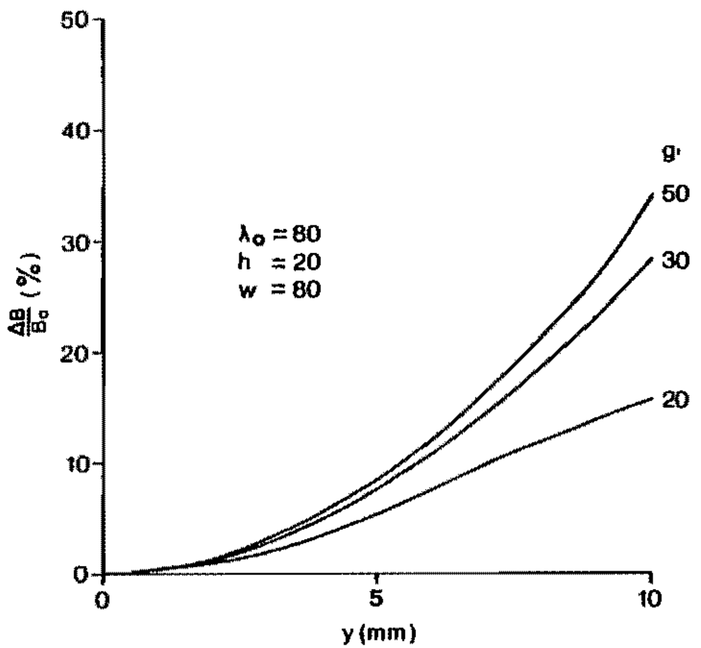
50
40
30
20
10
0
$\frac{\Delta B}{B_o}$ (%)
λ_o = 80
h = 20
w = 80
g:
50
30
20
0
5
10
y (mm)

Fig. 15

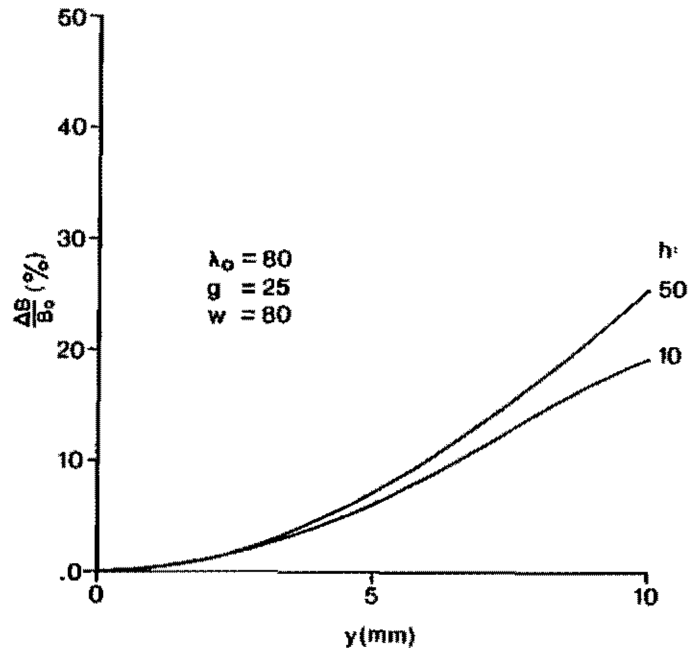
50
40
30
20
10
.0
$\frac{\Delta B}{B_o}$ (%)
λ_o = 80
g = 25
w = 80
h:
50
10
0
5
10
y (mm)

Fig. 16

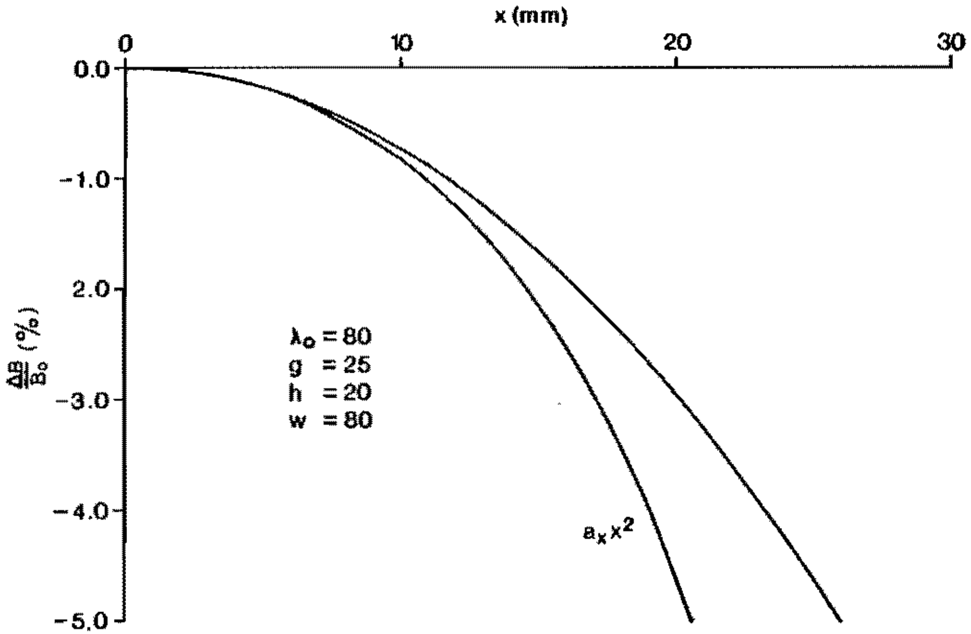
x (mm)
0
10
20
30
0.0
-1.0
2.0
-3.0
-4.0
-5.0
$\frac{\Delta B}{B_o}$ (%)
$\lambda_o = 80$
$g = 25$
$h = 20$
$w = 80$
$a_x x^2$

Fig. 17

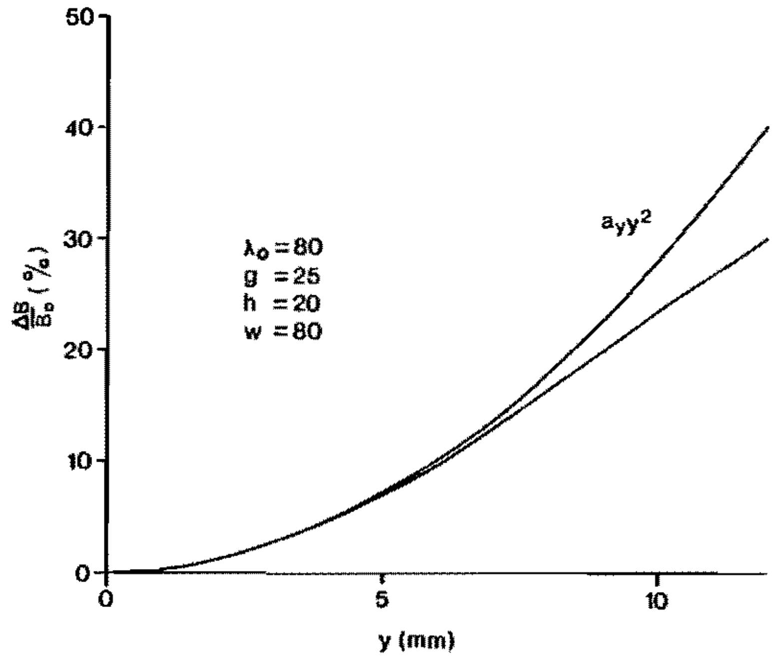
50
40
30
20
10
0
$\frac{\Delta B}{B_o}$ (%)
$\lambda_o = 80$
$g = 25$
$h = 20$
$w = 80$
$a_y y^2$
0
5
10
y (mm)

Fig. 18

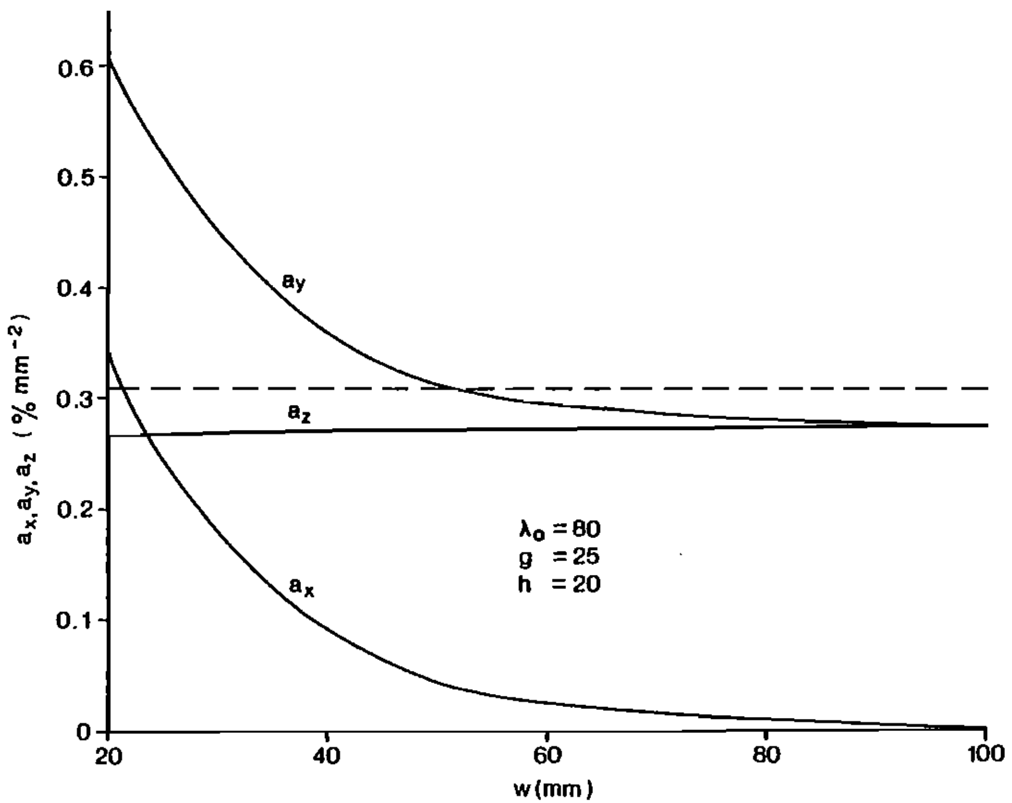

0.6
0.5
0.4
0.3
0.2
0.1
0
a_x, a_y, a_z (% mm^{-2})
a_y
a_z
a_x
$\lambda_o = 80$
$g = 25$
$h = 20$
20
40
60
80
100
w(mm)

Fig. 19

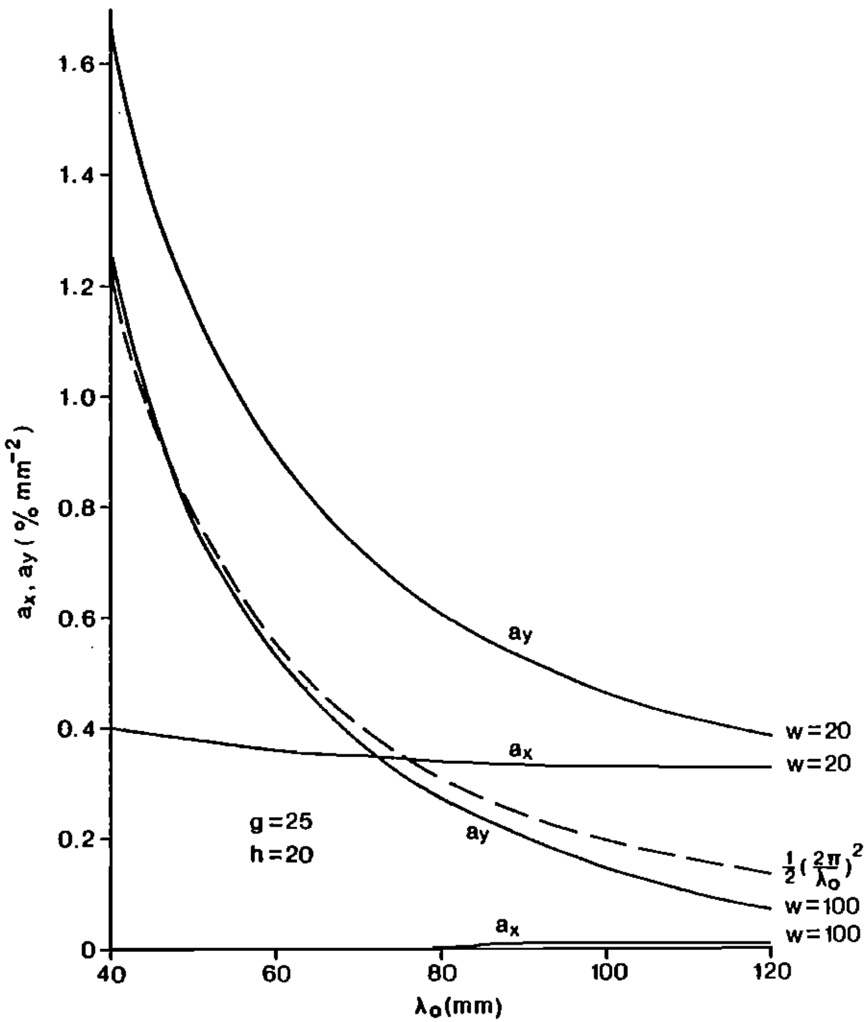

1.6
1.4
1.2
1.0
0.8
0.6
0.4
0.2
0
a_x, a_y (% mm^{-2})
a_y
a_x
a_y
a_x
w=20
w=20
$\frac{1}{2}(\frac{2\pi}{\lambda_o})^2$
w=100
w=100
g=25
h=20
40
60
80
100
120
λ_o(mm)

Fig. 20

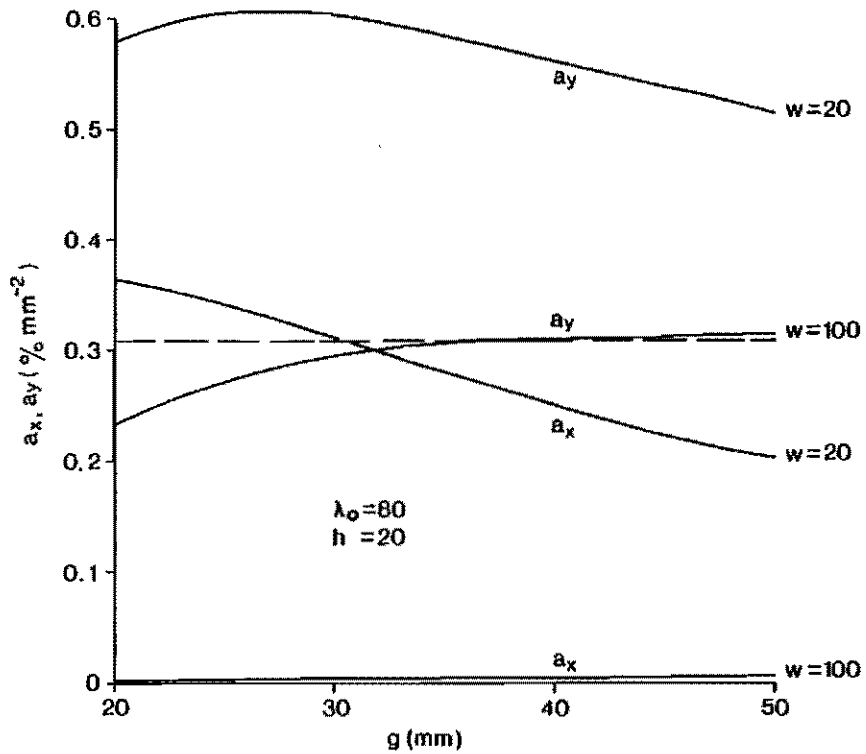
0.6
0.5
0.4
0.3
0.2
0.1
0
a_x, a_y (% mm^{-2})
a_y
w=20
a_y
w=100
a_x
w=20
λ_o=80
h =20
a_x
w=100
20
30
40
50
g (mm)

Fig. 21

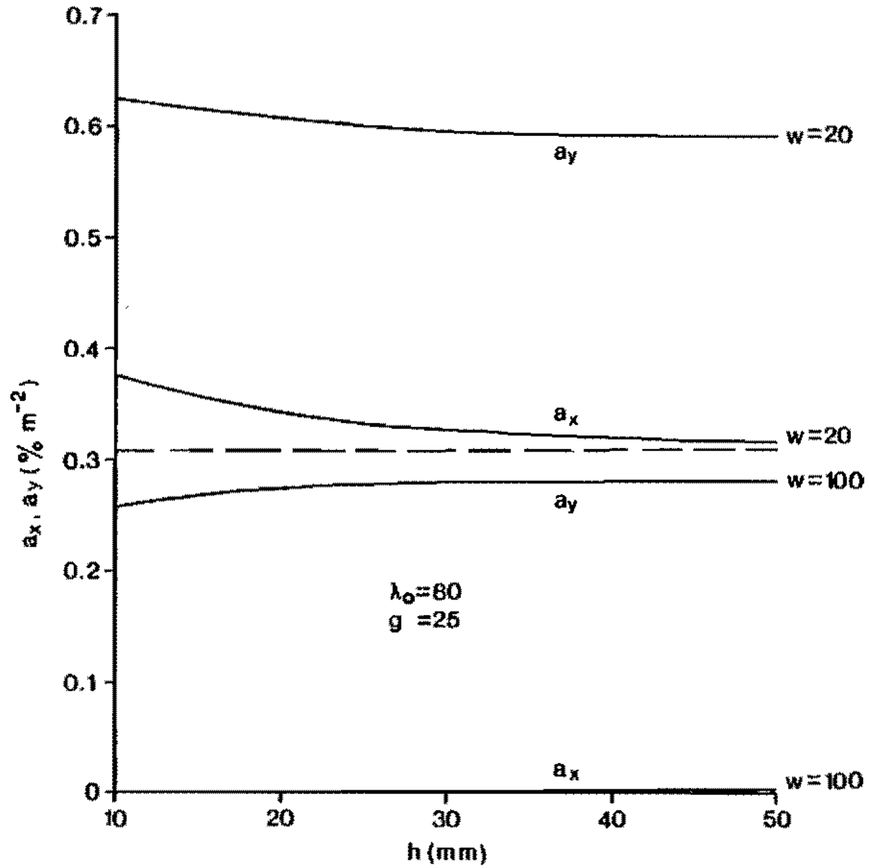
0.7
0.6
0.5
0.4
0.3
0.2
0.1
0
a_x, a_y (% m^{-2})
a_y
w=20
a_x
w=20
w=100
a_y
λ_o=80
g =25
a_x
w=100
10
20
30
40
50
h (mm)

Fig. 22

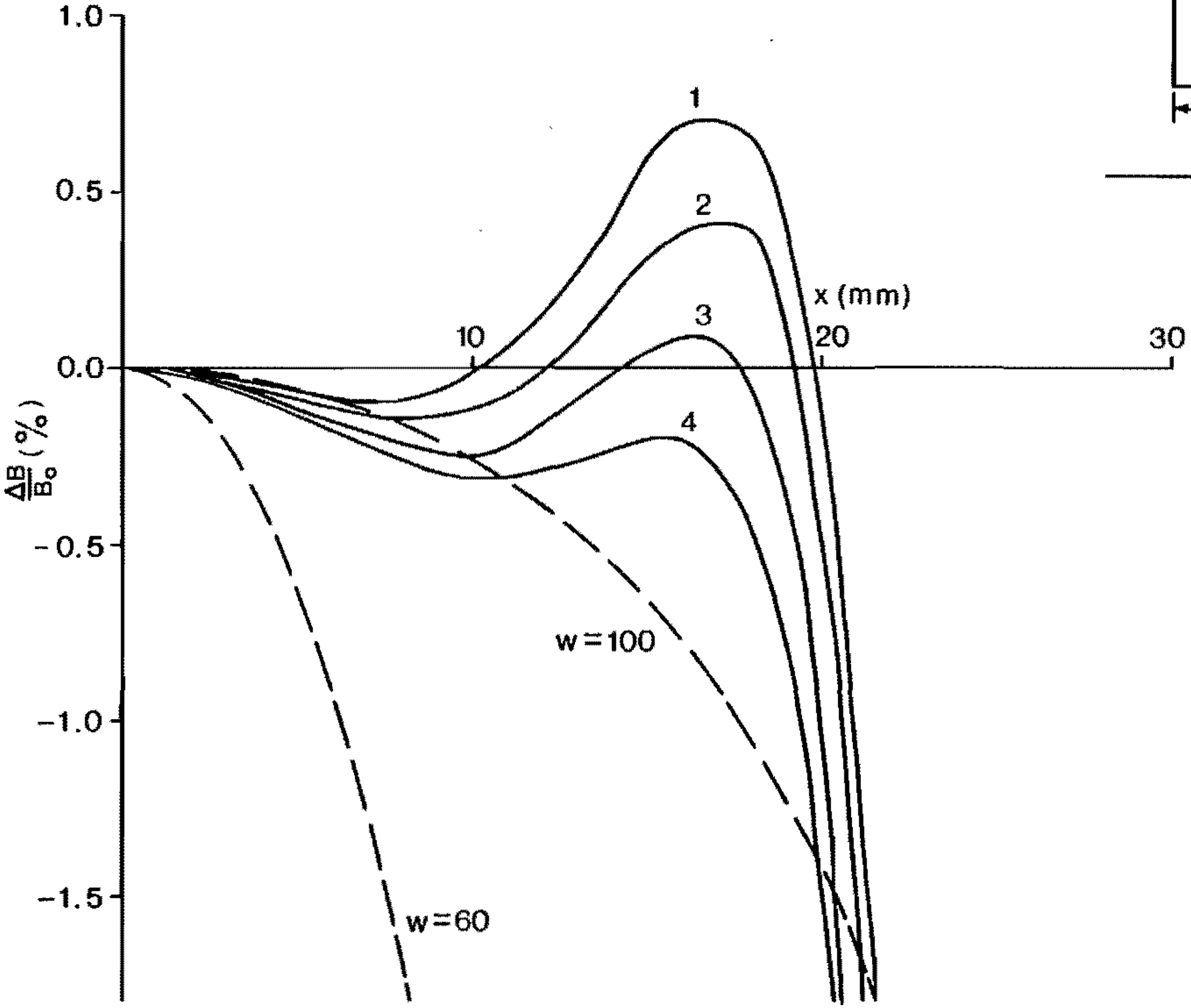

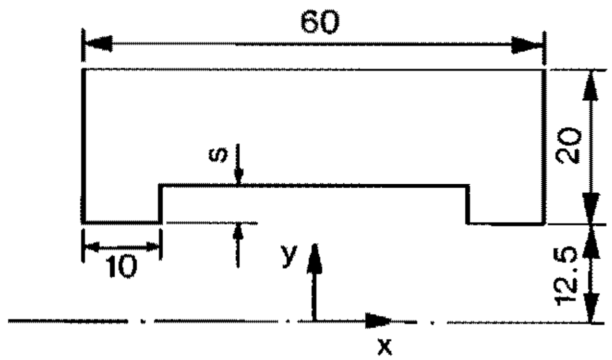

	s (mm)
1	3.9
2	3.8
3	3.7
4	3.6

Fig. 23

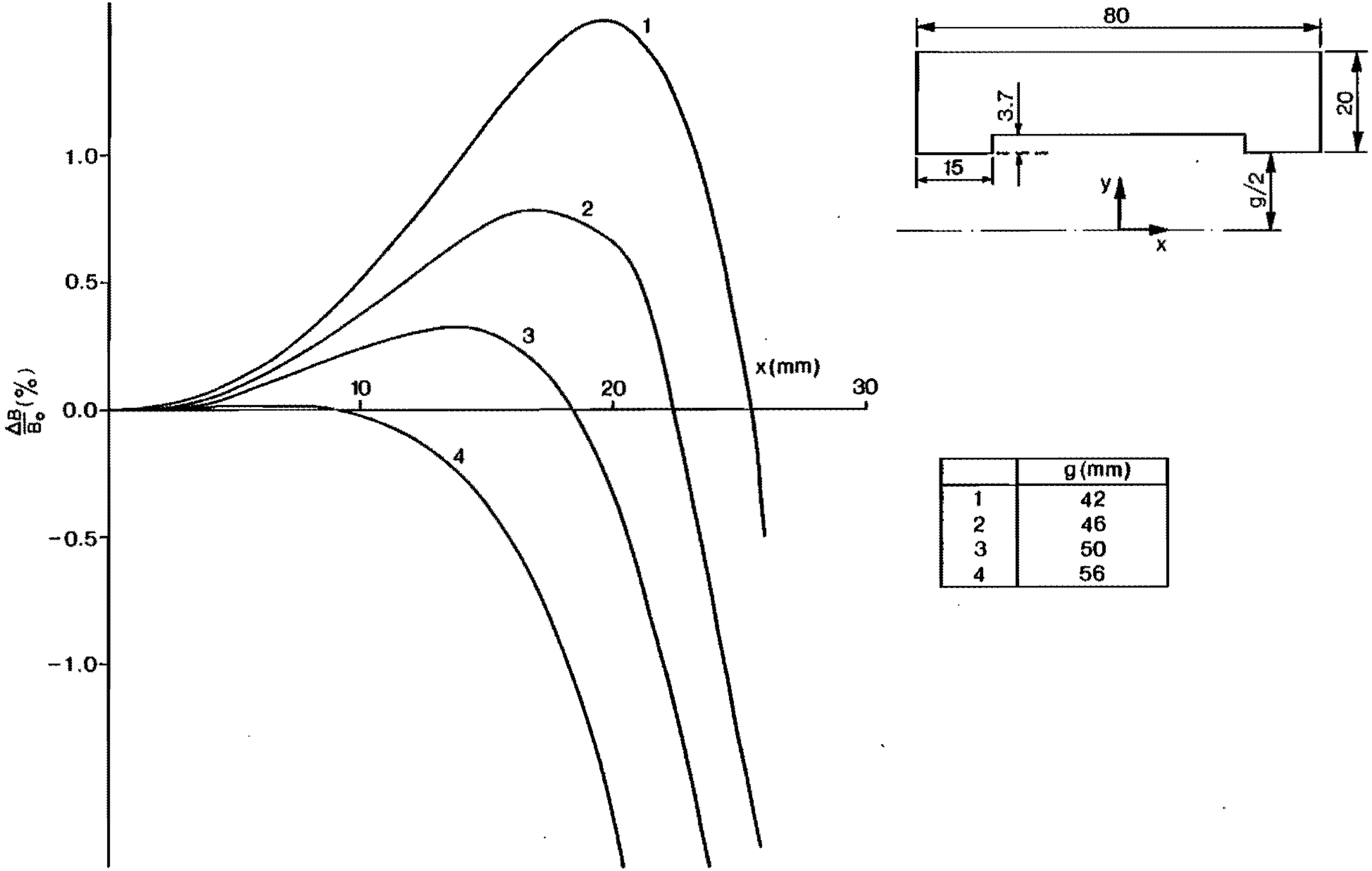

	g (mm)
1	42
2	46
3	50
4	56

Fig. 24

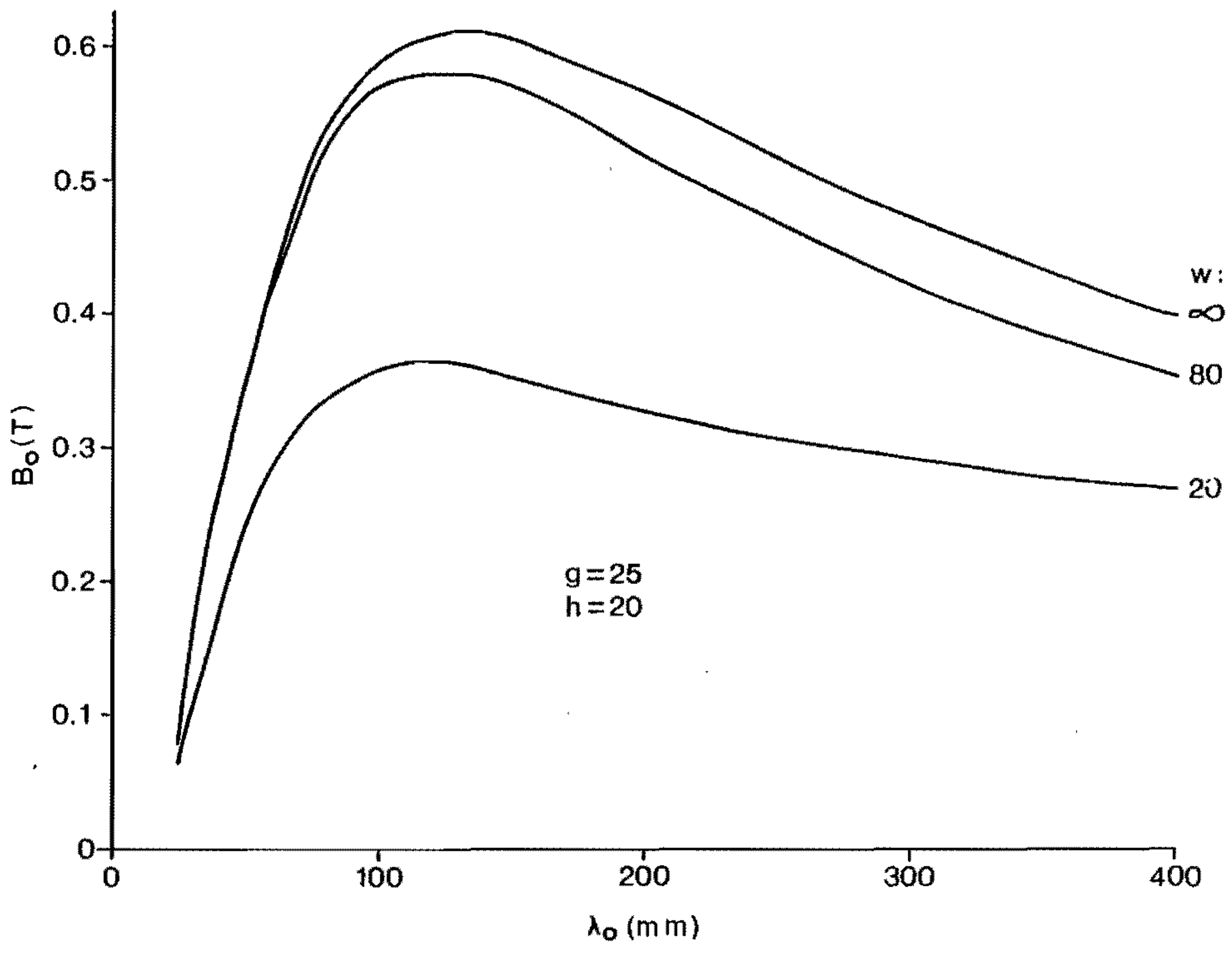

Fig. 25

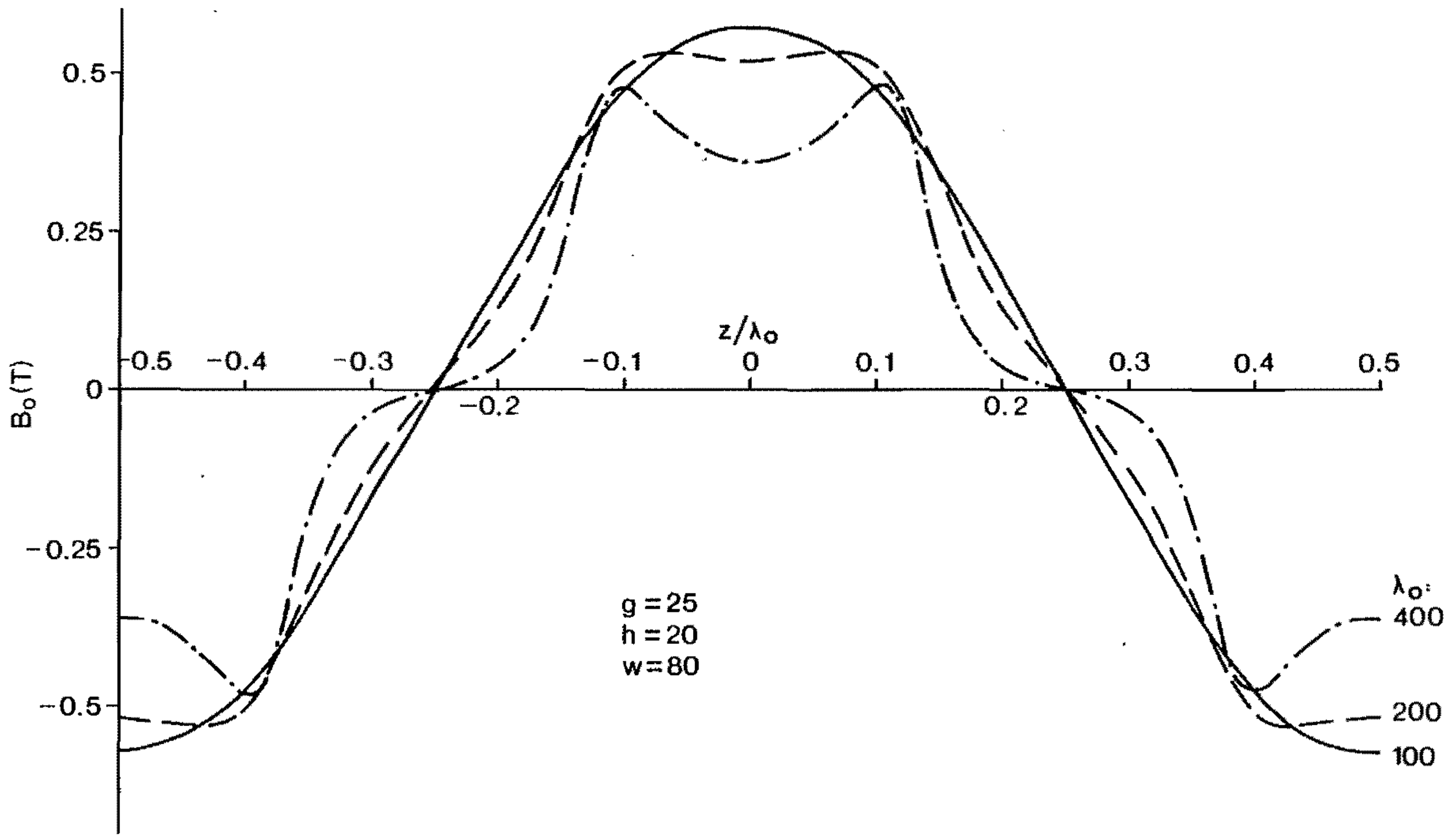
B₀(T)
0.5
0.25
0
−0.25
−0.5
z/λ₀
−0.5
−0.4
−0.3
−0.2
−0.1
0
0.1
0.2
0.3
0.4
0.5
g = 25
h = 20
w = 80
λ₀:
400
200
100

Fig. 26